Check for updates

Using stable isotopes in deciphering climate changes from travertine deposits: the case of the *Lapis Tiburtinus* succession (Acque Albule Basin, Tivoli, Central Italy)

Alessandro Mancini[1]*, Irene Cornacchia[2], Joachim Lamal[3†],
Enrico Capezzuoli[4], Rudy Swennen[3] and Marco Brandano[1,2]

[1]Department of Earth Sciences, University of Rome "Sapienza", Rome, Italy, [2]Italian National Research
Council-Institute of Environmental Geology and Geoengineering (CNR-IGAG), at Department of Earth
Sciences, University of Rome "Sapienza", Rome, Italy, [3]Geology, Earth and Environmental Sciences, KU
Leuven, Heverlee, Belgium, [4]Department of Earth Sciences, University of Florence, Florence, Italy,

Quaternary stable isotope records of marine and lacustrine carbonate deposits
as well as speleothems were extensively studied to reconstruct global and
regional climatic evolution. This study demonstrates how stable isotope
records of travertine provide fundamental information about climate and
the consequences of its evolution on groundwater level fluctuations. The
deposition of the *Lapis Tiburtinus* travertine succession occurred during the Late
Pleistocene (150−30 ka), coeval with the last activity of the Colli Albani volcanic
complex. Two boreholes (Sn1 and Sn2) were drilled into the Acque Albule Basin
(23 km E of Rome), crossing the entire *Lapis Tiburtinus* succession. The Sn1
borehole in the central part of the basin crosscuts a travertine succession of
62.1 m in thickness, while the Sn2 borehole in the southern part of the basin
is characterized by a travertine succession 36.3 m in thickness. Carbon and
oxygen stable isotope ratios were analysed on 118 samples (59 samples both for
Sn1 and Sn2 boreholes) representative of the entire *Lapis Tiburtinus* travertine
succession crossed by the boreholes. Values, measured and correlated in the
two drilled boreholes, permitted determination of the sensitivity of the travertine
depositional system to glacial and interglacial cycles, unravelling the complex
oxygen and carbon cycle dynamic recorded in such sedimentary succession.
Moreover, the results obtained correlated with available pollen curves of the
Mediterranean area (from the Castiglione crater, 25 km E of Rome). Regional
and global oxygen isotope continental and marine curves, calibrated with the
stratigraphy of the Acque Albule Basin, and available U/Th dating allow the
identification of at least three phases of the last interglacial (Marine Isotope Stage
5-MIS5). The carbon isotope record, compared with CO_2 flux reconstructed
and associated with the volcanic activity of the Colli Albani volcanic complex,
instead shows an influence from groundwater level changes. In particular,
positive shifts that occurred during arid phases are associated with a lower
groundwater level and increased CO_2 degassing, inducing a major fractionation
effect on carbon isotopes. Instead, the negative shifts occurring during more

humid periods indicate the inhibition of CO_2 degassing and increase in pressure, attesting to a rise in groundwater level. In this view, travertine deposits, frequently studied to define the tectonic setting and activity of the area where they develop, can thus also be used as a tool to understand climate changes and groundwater variations apparent in their stable oxygen and carbon isotope signature.

1 Introduction

The global triggers of glacial and interglacial cycles during the Quaternary have been largely established. However, little is still known about local responses to such global controlling factors, as well as the relationships between the latter and regional causes (Regattieri et al., 2015). Travertine deposits, controlled by climate, tectonic, and volcanic activity, thus represent the best archive for investigating these dynamics (Mancini and Capezzuoli, 2024). The term "travertine" is derived from the Italian *travertino*. It is related to the Latin words *Lapis Tiburtinus*, meaning "stone of Tibur," representative of the Roman name for the present-day village of Tivoli. Such material was quarried by the Romans in the Tivoli area and was mostly used as ornamental and building stone (e.g., the Colosseum, AD 70–80) from the first century BC. Travertine corresponds to calcium carbonate deposits related to non-marine waters supersaturated in calcium bicarbonate-rich waters and associated with hydrothermal fluid circulation (Chafetz and Folk, 1984; Pedley, 2009; Jones and Renaut, 2010; Capezzuoli et al., 2014; Mancini et al., 2019a; Mancini et al., 2019b; Mancini et al., 2019c; Mancini et al., 2021). In recent decades, travertine deposits have attracted a variety of scientific interest for different reasons as they are widespread in continental settings and important archives of palaeo-environmental proxies and also because they offer the possibility of reconstructing past ecosystems, tectonic settings, and sedimentary regimes of the environment in which they developed (Capezzuoli et al., 2014; Brogi et al., 2018). Moreover, these deposits could also be used to address the relationships between deposition and related bacterial activity as a proxy for geogenic/biogenic CO_2 fluxes associated with the precipitation of calcium carbonate deposits and as reservoir analogues for hydrocarbon reservoirs (Claes et al., 2015, 2016; Ronchi and Cruciani, 2015; Schröder et al., 2016; Mancini et al., 2019a; Mancini et al., 2020). However, identifying in detail the impact of climate changes in different depositional settings and understanding the interplay between global, regional, and local trends that potentially affect a depositional system are always a challenging frontier for geosciences. Hence, travertine deposits represent a particularly interesting case study, as their deposition is controlled by a complex set of physical, chemical, and biological processes (Della Porta, 2015; Della Porta et al., 2017a), particularly influenced by the local tectonic setting in which they develop (Hancock et al., 1999; Capezzuoli et al., 2014; Brogi et al., 2021a; Brogi et al., 2021b). Despite their complexity, recent studies have hypothesized climatic control of travertine precipitation (Frank et al., 2000; Crossey et al., 2006; Uysal et al., 2007; Faccenna et al., 2008; Uysal et al., 2009; Brogi et al., 2010; Anzalone et al., 2017; Ricketts et al., 2019; Giustini et al., 2020).

Faccenna et al. (2008) noticed that the onset of the *Lapis Tiburtinus* travertine deposition in the Acque Albule Basin was coeval with the last interglacial of the Late Pleistocene (MIS5 *sensu* Shackleton, 1969; Ruddiman, 2006), starting at the onset of the last interglacial ca 115 ka and ending at the beginning of the last glaciation, 30 ka ago. Moreover, Anzalone et al. (2017), analysed the oxygen isotope record on a 30-m thick *Lapis Tiburtinus* travertine core and noted a precessional control on the travertine deposition.

Travertine deposition can be influenced by global changes in climate (Ricketts et al., 2019). However, despite the singular attempt by Ricketts et al. (2019) to correlate the oxygen isotope record of travertine to global trends, no other studies have investigated the potential of travertine systems to record climate changes since most of the abundant literature focuses on the endogenic causes leading to travertine deposition (Crossey et al., 2006; Uysal et al., 2007, 2009; Brogi et al., 2010; Faccenna et al., 2008; De Filippis et al., 2013; Castorina et al., 2023) than on external forcing (Frank et al., 2000; Mancini et al., 2021).

In addition, travertine systems are extremely heterogeneous in terms of lateral facies changes, even considering the relatively spatially limited settings of precipitation. This characteristic feature of travertine often hampers the possibility of correlating different records even over small distances and probably discourages the development of significant paleoclimate studies on these peculiar settings. In this paper, we address this frontier challenge, focusing our attention on the *Lapis Tiburtinus* travertine succession of the Acque Albule Basin, Tivoli, central Italy (Faccenna et al., 2008; Della Porta et al., 2017b; Mancini et al., 2021), to explore the sensitivity of travertine systems to global climate changes. In particular, the aims of the paper are threefold: 1) to evaluate the potential of travertines to record global oxygen isotope shifts and, thus, glacial and interglacial cycles; 2) to identify the relationship between global forcing and the local controlling factors on travertine precipitation through the comparative study of oxygen and carbon isotope ratios; 3) to evaluate the carbon isotope record associated with the groundwater level changes compared with CO_2 flux and volcanic activity of the Colli Albani volcanic complex.

2 Geological setting

The Acque Albule Basin represents the eastern part of the Roman Basin, bounded to the north and east by the Neogene Apennine fold and thrust belt (i.e., Cornicolani–Lucretili–Tiburtini Mountains), by the Aniene River and Pleistocene Colli Albani volcanic complex to the south, and by the Tiber River valley to the west

(Figure 1A). The extensional tectonic activity that occurred during the Pliocene–Quaternary interval controls the basin's evolution (Conato et al., 1980; Faccenna et al., 2008; De Filippis et al., 2013; Della Porta et al., 2017b; Cardello et al., 2022). The eastern side of the Apennine belt is characterized by Meso-Cenozoic carbonate rocks that form thrust sheets with a piggy-back sequence from the Late Miocene to the Pliocene epochs, while the western side is influenced by extensional tectonic activity occurring from the Middle Miocene to the Pliocene and related to the opening of the back-arc basin (Tyrrhenian Sea) (Funiciello et al., 1976; Chiodini et al., 2004; Acocella and Funiciello, 2006; Rossetti et al., 2007; Mancini et al., 2014). The Acque Albule Basin (Figure 1B) is located 30 km east of Rome and is characterized by a flat topography (Faccenna et al., 2008; De Filippis et al., 2013; Di Nezza et al., 2015; Anzalone et al., 2017). The morphological depression of the Acque Albule Basin is influenced by moderate subsidence of 0.4 mm/yr (Faccenna et al., 2008; De Filippis et al., 2013) and is controlled by Pleistocene–Holocene tectonic activity mainly associated with N–S-striking right-lateral and transtensional to normal faults (Cosentino and Parotto, 1986; Corrado et al., 1992; Faccenna et al., 1994; Gasparini et al., 2002; Billi et al., 2006; Faccenna et al., 2008; De Filippis et al., 2013). The succession filling the Acque Albule Basin is related to Plio-Pleistocene alluvial, lacustrine, and epivolcanic deposits that accumulated on top of a Meso-Cenozoic marine carbonate succession (De Rita et al., 1995; La Vigna et al., 2013a; La Vigna et al., 2013b). On top the Plio-Pleistocene deposits a travertine succession developed. Known as *Lapis Tiburtinus* travertine, this carbonate developed during the Late Pleistocene (115–30 ka) and covers an area of 28 km^2 with a maximum thickness of 90 m (Faccenna et al., 2008). The *Lapis Tiburtinus* travertine succession is characterized by bedded to sub-horizontal units with onlapping geometries on the underlying erosional surfaces dipping toward the south, east, and west and separated by erosional surfaces covered by palaeosoils and conglomerate deposits (less than 1 m) (Faccenna et al., 2008; De Filippis et al., 2013). The Acque Albule Basin and its hydrogeological regime are influenced by the presence of the Meso-Cenozoic carbonate succession to the north, northeast, and east of the basin (Cornicolani–Lucretili–Tiburtini Mountains) (Carucci et al., 2012; La Vigna et al., 2013a, La Vigna et al., 2013b) and by the damage zone associated with the N–S striking faults (Billi et al., 2006) that affect these deposits. Three different hydrostratigraphic units comprise the local groundwater conceptual flow model (Carucci et al., 2012; La Vigna et al., 2013a; La Vigna et al., 2013b). From base to top, 1) the first is related to the Meso-Cenozoic limestone of the Apennine belt, cropping out in the surrounding area of the basin and lowered by the activity of normal faults, 2) the second unit, developed on top of the Meso-Cenozoic limestone, is characterized by Pliocene–Pleistocene sand-claystone marine deposits, and 3) the third is represented by the fractured travertine deposits, strongly affected by anthropogenic activities. Several CO$_2$-rich thermal springs, mainly located close to the N–S-striking right-lateral faults, are characterized by a temperature of 23 °C and pH values between 6.0 and 6.2, while the Aniene River, located to the south of the basin, is the main run-off destination of all the superficial thermal waters (Pentecost and Tortora, 1989; Minissale et al., 2002; Minissale, 2004; Carucci et al., 2012; La Vigna et al., 2013a; La Vigna et al., 2013b; Di Salvo et al., 2013).

3 Materials and methods

Two boreholes (Sn1 and Sn2) crossing the entire *Lapis Tiburtinus* travertine succession of the Acque Albule Basin (Figures 2A, B) were drilled with a Beretta T47S. The Sn1 borehole was drilled in the north-west of the quarried area to a depth of 70 m, while the Sn2 borehole, located in the south of this area, reached a depth of 42 m. The quarried area lies in a topographic depression, with a topographical height of 31–78 m above sea level. The top of the Sn1 borehole occurs at 68.2 m above sea level, while the Sn2 borehole is situated at 57.4 m. A detailed core description of both the Sn1 and Sn2 cores was carried out which focused on macroscopic characteristics. Nine different lithofacies associations were recognized: six related to travertine deposits and four to non-travertine deposits (Figures 3A–I). For lithofacies identification and description, we refer to Mancini et al. (2021). The age constraints used for dating and mutual correlations are from Faccenna et al. (2008), while the geogenic CO$_2$ fluxes associated with travertine depositional units are based on Mancini et al. (2020). The CO$_2$ discharge rate was obtained by dividing the CO$_2$ discharge by the area of the hydrological basin that feeds the springs. From both cores, a total of 59 (118) pure calcite powder samples, collected every 2–2.5 m on average, were acquired by a dental drill. Visible crystalline cements were avoided. Stable oxygen and carbon isotopic signatures were determined at the Friedrich-Alexander-Universität (Erlangen–Nürnberg, Germany). Carbonate powders were analysed with a Thermo Finnigan V and mass spectrometer (Thermo Scientific Inc.), coupled with a Gasbench II device, after attacking them with 100% phosphoric acid at 70 °C. The analytical standard deviations for δ^{13}C and δ^{18}O are 0.04‰ and 0.05‰, respectively. The values obtained are reported in per mil (‰), relative to Vienna Pee Dee Belemnite (V-PDB), by assigning a δ^{13}C value of +1.95‰ and a δ^{18}O value of −2.20‰ to the standard NBS19.

4 Results

4.1 Lithofacies

The classification and characterization of the different deposits observed in the Sn1 and Sn2 cores are reported in Table 1. The different lithofacies types are subdivided into "travertine" and "non-travertine" deposits (see also Figures 2, 3).

4.2 Depositional units, travertine volume, and geogenic CO$_2$ fluxes

The Acque Albule Basin covers 28 km^2, while travertine deposits have a total volume of 1.1 km^3 and can be divided into 10 different depositional units labelled "U1" to "U10" from base to top (Table 2 and also Figure 2) (Faccenna et al., 2008; De Filippis et al., 2013). The travertine succession studied in the Sn1 and Sn2 cores develops on top of different clastic deposits. In the Sn1 core, travertine succession occurred on top of claystone and marlstone deposits related to lacustrine and alluvial plain depositional environments,
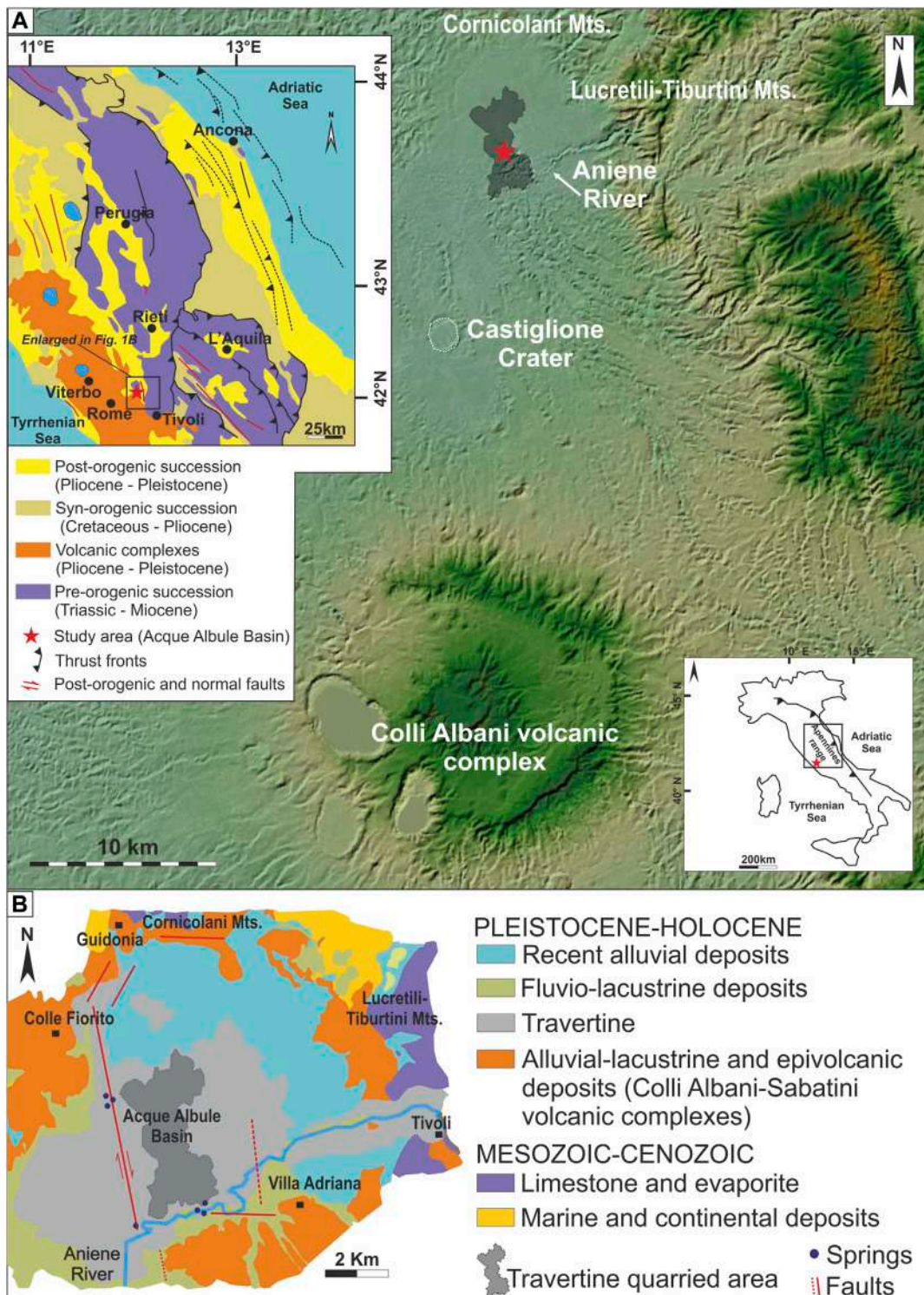
FIGURE 1
(A) Geological map of Central Italy with an indication of the study area (square) and a digital elevation model of the study area (modified from Tarquini et al., 2023). (B) Geological map of the Acque Albule Basin (modified from Mancini et al., 2021).

while the travertine succession of the Sn2 core developed on top of fluvial sand, sandstone, and conglomerates related to a fluvial depositional environment in relation to the activity of the Aniene River. The 10 depositional units were correlated in both Sn1 and

Sn2 cores based on Erthal et al. (2017), Della Porta et al. (2017b), and Mancini et al. (2021) and were integrated with the previous subdivision and age dating reported by Faccenna et al. (2008). The following units were differentiated:
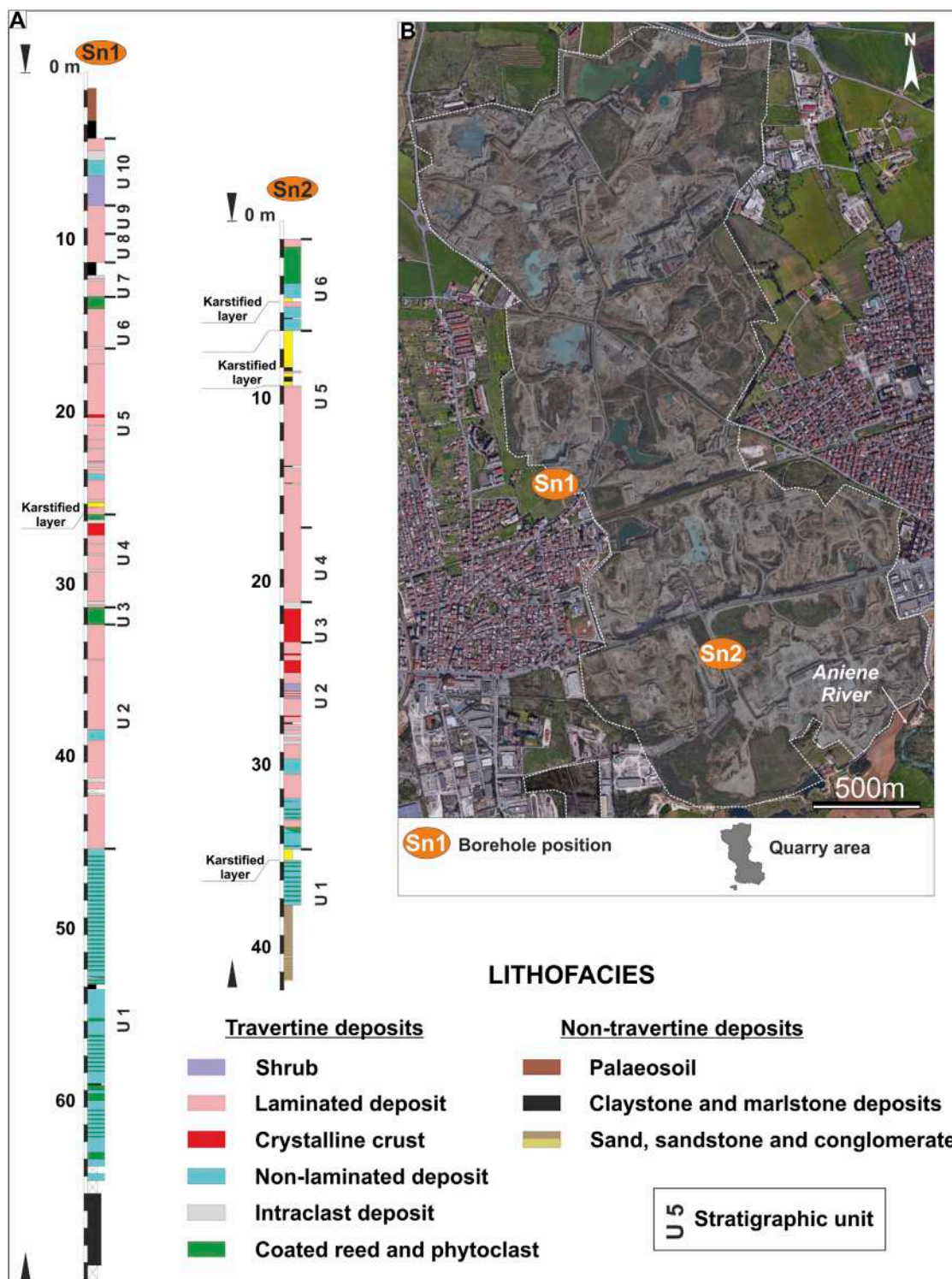
FIGURE 2
(A) Stratigraphic log and pictures of Sn1 and Sn2 boreholes showing the lithofacies, divided in travertine and non-travertine deposits, and depositional units; **(B)** map showing positions of Sn1 and Sn2 boreholes (modified from Google Earth, 2023).

- Unit 1 is the first travertine depositional event in the studied boreholes. In the Sn1 core, this unit is 20 m thick, while Sn2 is only 3 m thick. Claystone layers rich in pyrite are interdigitated with non-laminated lithofacies in the Sn1 core, while, in Sn2,

Unit 1 is composed exclusively of non-laminated travertine lithofacies. Such lithofacies association testifies to deposition in a low-energy setting such as a pool or shallow lake with freshwater input which was sometimes affected by anoxic

FIGURE 3
(A–I) Pictures showing the different lithofacies related to travertine and non-travertine deposits. **(A)** Laminated deposit; **(B)** shrubs; **(C)** intraclast deposit; **(D)** crystalline crust; **(E)** coated reed and phytoclast; **(F)** non-laminated deposit; **(G)** palaeosoil; **(H)** sand, sandstone, and conglomerate; **(I)** claystone and marlstone deposits; **(J,K)** pictures showing the characteristics of the karstified travertine deposits observed in the Sn2 borehole.

conditions. This unit was deposited between 115 ± 5 and 99 ± 5 ka with a travertine volume deposit of 0.16 km^3 associated with a geogenic CO_2 flux of 1.11×10^6 mol a^{-1} km^{-2}.

- Unit 2 has a thickness of 13 m in Sn1 and 11.2 m in Sn2. Non-laminated deposits vertically alternating with laminated and intraclast deposit lithofacies occurred in Sn1, while coated reed and phytoclast, laminated deposit, intraclast deposit, non-laminated deposit, shrub, crystalline crust, and claystone and marlstone deposits are observable in Sn2. This lithofacies association suggest a subaqueous depositional environment in the Sn1 borehole and a palustrine setting with freshwater input in Sn2.

- Unit 3 has a thickness of 1.3 m in the Sn1 core and 2.2 m in Sn2. Laminated deposits associated with intraclast deposits and coated reed and phytoclast lithofacies are predominant in Sn1, while crystalline crust and intraclast deposits occur in Sn2. The

TABLE 1 Description of the travertine and non-travertine lithofacies associations observed in the Sn1 and Sn2 cores.

Travertine lithofacies	Description	Depositional environment
Shrub	Clotted peloidal micrite dendrite boundstone layers. Sometimes coated grains, coated bubbles, and raft layers occur interbedded	Shallow lakes, pools, and ponds
Laminated deposit	Laminated micrite boundstone, mudstone, and packstone-forming layers frequently associated with coated grains, aggregates of clotted peloidal micrites, coated bubbles, rafts, and intraclasts	Shallow lakes, pools, and ponds
Crystalline crust	Crystalline fan dendritic cementstone and cruststone. The crystalline fans, composed of calcite, have a millimetre to centimetre dimension	Slope and rims
Non-laminated deposit	Packstone and mudstone with coated reed stems, *Charophytes*, gastropod shells, ostracods, and intraclasts	Pools, shallow lakes, and ponds with the input of freshwater
Intraclast deposit	Floatstone, packstone, and rudstone with angular intraclast with a metre to centimetre dimension	Pools
Coated reed and phytoclast	Phytothermal boundstone to phytoclastic packstone with coated reed stems, *Charophytes*, gastropod shells, and rafts	Environment affected by the input of freshwater. Distal part of ponds, pools, and shallow lakes
Non-travertine lithofacies	**Description**	**Depositional environments**
Palaeosoil	Immature brown palaeosoils rich in clay. Sometimes bones, root moulds, and gastropod shells are observable	Pedogenized substrate
Claystone and marlstone deposits	Clay, marl, and silt. Pyrite crystals and gastropod shells are sometimes observable but sparse in the matrix	Shallow lakes, pools, and ponds
Sand, sandstone and conglomerate	Polymictic and monomictic conglomerates with rounded and sub-rounded clasts of travertine and marine limestone of the Lucretili and Tiburtini mountain ranges. Grey-green sandstones with cross-bedding are observed	Fluvial channels and rivers

lithofacies association suggests subaqueous conditions in Sn1 and a slope setting in Sn2.

- Unit 4 has a thickness of 5 m in Sn1 and 4.5 m in Sn2. Laminated deposits interbedded with intraclast lithofacies occur in Sn1, while, in Sn2, laminated deposit is interbedded with crystalline crust, intraclast deposit, coated reed, and phytoclast lithofacies. Based on the lithofacies associations, the deposition occurred in a subaqueous environment (Sn1) passing to a slope setting (Sn2).
- Unit 5 has a thickness of 9.6 m in Sn1 and 10.4 m in Sn2. In Sn 1, it is composed of laminated deposit, shrub, non-laminated deposit, intraclast deposit, and crystalline crust lithofacies association. In Sn2, however, the lithofacies association is characterized by the presence of laminated, intraclast claystone, and marlstone deposits. In both cores, the lithofacies association suggests a depositional environment mainly characterized by subaqueous conditions and a slope setting.
- Unit 6 is 3 m thick in Sn1 and 5 m in Sn2. Laminated deposits, associated with intraclast deposit and coated reed and phytoclast lithofacies, are observable in Sn1, while the presence of non-laminated deposits, and coated reed and phytoclast

laminated deposits, as well as claystone and marlstone deposits, characterize Unit 6 in Sn2. Both lithofacies associations of Sn1 and Sn2 attest to subaqueous deposition.

Units 2–6 were deposited, according to Faccenna et al. (2008), from 99 ± 5 to 82 ± 9 ka, with a travertine volume of 0.31 km^3 associated with a geogenic CO_2 flux of 2.02×10^6 mol a^{-1} km^{-2}.

Units 7–10 were only recognised in Sn1 since these travertines had already been quarried at the Sn2 location.

- A thickness of 2 m characterizes Unit 7 in Sn1. Laminated and intraclast deposits as well as claystone and marlstone are the predominant lithofacies; this association attests to deposition in subaqueous and slope environments.
- Unit 8 is 1.9 m thick in Sn1. Laminated deposit is the predominant lithofacies, attesting to subaqueous deposition. Units 7 and 8 were deposited according to Faccenna et al. (2008) at a time interval between 82 ± 9 ka and 56.1 ± 1 ka, with a travertine volume of 0.21 km^3 associated with a geogenic CO_2 flux of 9.14×10^5 mol a^{-1} km^{-2}.
- Unit 9 is 1.5 m thick in Sn1 and is composed of laminated deposits, attesting to a subaqueous environment. This unit was

TABLE 2 Travertine depositional units of Sn1 and Sn2 boreholes, with thickness, lithofacies description, age, volume, and geogenic CO_2 fluxes calculated. The latter are reported based on Mancini et al. (2020).

Unit	Thickness m)		Lithofacies		Age (ka)	Volume (km^3)	φCO_2 (mol a^{-1} km^{-2})
	Sn1	Sn2	Sn1	Sn2			
U10	4.8	—	Laminated deposit, intraclast deposit, non-laminated deposit, and shrub	Quarried	44 ± 4–34 ± 5	0.34	2.70×10^6
U9	1.5	—	Laminated deposit	Quarried	56.1 ± 1–44 ± 4	0.08	7.11×10^5
U8	1.9	—	Laminated deposit	Quarried	82 ± 9–56.1 ± 1	0.21	9.14×10^5
U7	2	—	Laminated deposit, intraclast deposit, and claystone and marlstone deposit	Quarried			
U6	3	5	Intraclast deposit, laminated deposit, and coated reed and phytoclast	Non-laminated deposit, laminated deposit, coated reed and phytoclast, and claystone and marlstone deposit	99 ± 5–82 ± 9	0.31	2.02×10^6
U5	9.6	10.4	Laminated deposit, non-laminated deposit, shrub, crystalline crust, and intraclast deposit	Laminated deposit, intraclast deposit, and claystone and marlstone deposit			
U4	5	4.5	Laminated deposit, intraclast deposit, crystalline crust, and coated reed and phytoclast	Laminated deposit			
U3	1.3	2.2	Intraclast deposit, coated reed, and phytoclast and laminated deposit	Intraclast deposit and crystalline crust			
U2	13	11.2	Laminated deposit, non-laminated deposit, and intraclast deposit	Laminated deposit, non-laminated deposit, intraclast deposit, coated reed and phytoclast, crystalline crust, shrub, and claystone and marlstone deposit			
U1	20	3	Non-laminated deposits, coated reed and phytoclasts, intraclast deposits, claystone and marlstone deposits, and volcanoclastic deposit	Non-laminated deposits	115 ± 5	0.16	1.11×10^6

deposited between 56.1 ± 1 ka and 44 ± 4 ka (Faccenna et al., 2008) with a travertine volume of 0.08 km^3 associated with a geogenic CO_2 flux of 7.11×10^5 mol a^{-1} km^{-2}.

- The youngest stratigraphic unit, Unit 10, is 4.8 m thick in Sn1 and is mainly composed of shrub, laminated, intraclast, and non-laminated deposits, attesting to a subaqueous low-energy depositional setting (Scalera et al., 2021). This unit was deposited between 44 ± 4 ka and 34 ± 5 ka (Faccenna et al., 2008) with a total volume of 0.34 km^3 and is associated with a geogenic CO_2 flux of 2.70×10^6 mol a^{-1} km^{-2}.
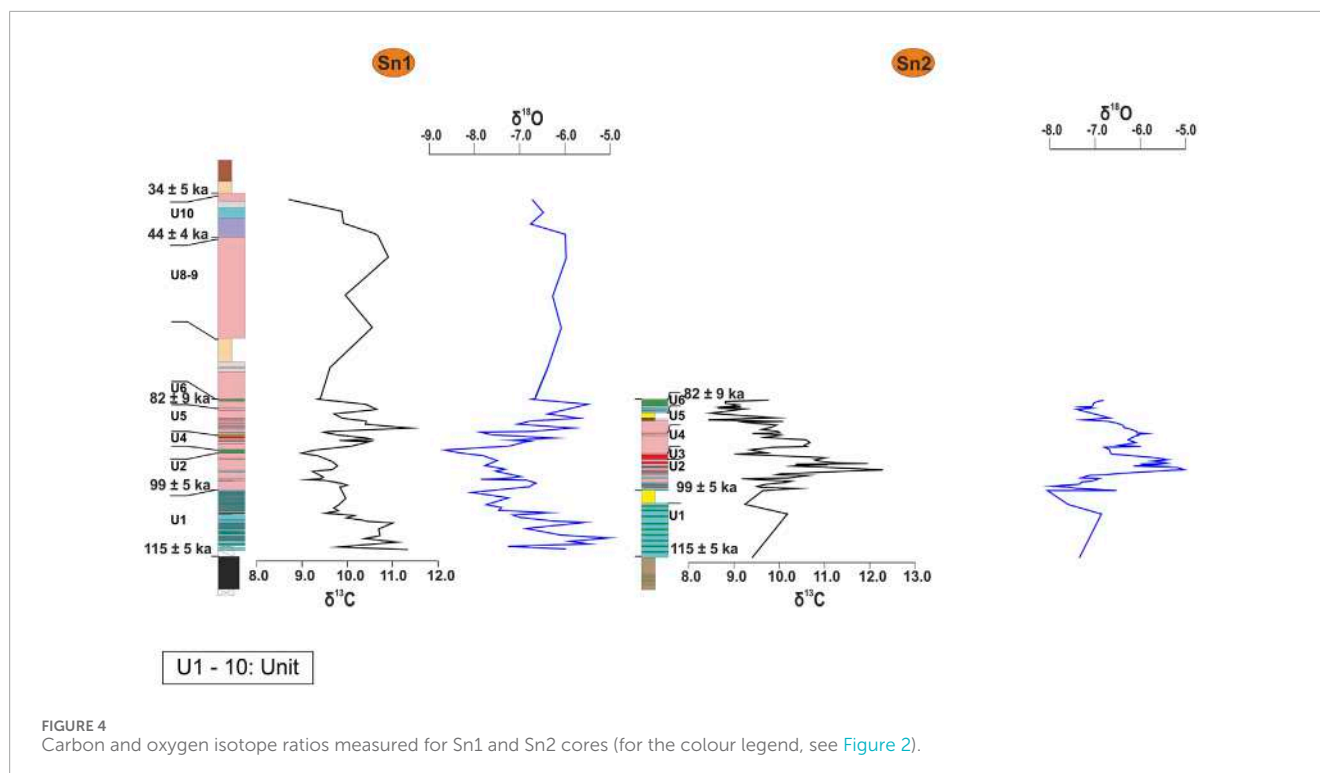
4.3 Carbon and oxygen stable isotopes

Figure 4 illustrates the $\delta^{13}C$ and $\delta^{18}O$ values of the Sn1 and Sn2 travertines.

In Sn1, the oxygen isotope ratios (Figure 4) are entirely negative, varying between −8.66‰ and −5.02‰. The base of the core shows a less depleted spike, with values rising from −7.26‰ at 63.25 m to −5.02‰ at 60.55 m, followed by a longer negative trend where the values lower to −8.06‰ at 45.95 m. A second less depleted

spike is then recorded, with values up to −6.64‰ at 42.73 m, followed by a depletion trend until 31.07 m, where a $\delta^{18}O$ of −8.66‰ is recorded, being the lowest of the entire section. Then, the highest portion of the core is characterized by a less depleted trend, with values rising to −5.47‰ at 15 m to mildly lower in the subsequent uppermost portion of the core, reaching −6.73‰ at 13.20 m. There, it remains rather stable up to the top of the core, where the last sample, recovered at −4.46 m, is characterized by a $\delta^{18}O$ of −6.71‰.

The carbon isotope (Figure 4) ratios in Sn1 are, instead, all significantly positive, spanning 8.70‰–11.36‰. The lowest portion of the core shows values scattered between 10‰ and 11‰, with no evident trend. Conversely, a trend can be identified between 55.58 m and 52.45 m, where the $\delta^{13}C$ evolves from 10.98‰ to 9.50‰ to subsequently oscillate between 9‰ and 10‰ up to 32.09 m. Then, a two-stepped shift is recorded, with values rising to 10.47‰ and 10.51‰, respectively at 28.10 m and 27.26 m, and then further up to 11.36‰ at 23.32 m, where the highest values are recorded. This positive shift is followed by a decrease in the carbon isotope ratios, which is lower to 9.34‰ at 13.20 m. Lastly, in the uppermost portion of the core, a sharp positive shift is recorded, characterized

FIGURE 4
Carbon and oxygen isotope ratios measured for Sn1 and Sn2 cores (for the colour legend, see Figure 2).

by values up to 10.88‰ at 8.36 m and then down to 8.70‰ at the top of the core.

In Sn2, the oxygen isotope ratios (Figure 4) are entirely negative, and span from −8.06‰ to −5.03‰. The base of the core shows an oscillation between −8.06‰ and −6.53‰. A wide shift towards less depleted values is then recorded, with values reaching −5.03‰ at 26.65 m. Then, a long negative shift is recorded up to 18.60 m, where a $\delta^{18}O$ of −6.79‰ is attested. A second minor isotope shift towards less depleted values is recorded in the upper part of the core, where the values rise to −5.86‰ at 13.59 m, followed by an isotope ratio decrease to −7.41‰ at 4.81 m. Lastly, the uppermost portion of the core shows again a rising trend to −6.81‰.

The carbon isotope ratios (Figure 4) are entirely positive, from 8.43‰ to 12.29‰. At the base of the core, the values oscillate between 9.17‰ and 10.38‰. From 29.90 m, a marked positive isotope shift starts, with values rising to 12.29‰ at 26.65 m to subsequently evolve to 9.01‰ at 20.98 m. Then, a second minor, positive carbon isotope shift is recorded, with values rising to 10.68‰ at 18.60 m. Then, a general decrease towards lighter values is attested, with values down to 8.43‰ at 8.70 m. The uppermost portion of the core does not show particular trends, where wide oscillations of the $\delta^{13}C$ values between 8.43‰ and 9.90‰ can be seen.

5 Discussion

Reported carbon and oxygen isotope ratios of the two analysed Sn1 and Sn2 cores agree with previously published isotope data on the *Lapis Tiburtinus* travertine succession/hydrothermal system (Minissale et al., 2002; Anzalone et al., 2017; Della Porta et al., 2017b). In particular, the oxygen isotope record attests to

a hydrothermal origin, probably influenced by precipitation temperatures of thermal water and original isotopic water composition (Della Porta et al., 2017b). Such values are coherent with those measured in Central Italian travertine deposits (Minissale et al., 2002; Della Porta et al., 2017b). Furthermore, the carbon isotope signature of the *Lapis Tiburtinus* travertine succession is significantly heavier than known Pleistocene–Neogene Italian travertine systems, as already observed by Minissale et al. (2002) and Della Porta et al. (2017b). The 2‰–4‰ heavier carbon isotope values of the *Lapis Tiburtinus* travertine succession are related to different factors, such as pH, isotopic composition of the dissolved inorganic carbon, mixing with meteoric water percolating through soil, carbon isotope values of the carbonate bedrock, the distance from the hydrothermal springs, and by downstream CO_2 degassing processes (Della Porta et al., 2017b). Moreover, according to Minissale et al. (2002), the heavier carbon isotope values measured for the *Lapis Tiburtinus* travertine succession reflect the typical CO_2 signal related to the metamorphism of the Meso-Cenozoic marine limestone substrate and/or derived from magmatic to mantle sources. The mantle source derivation is also testified by the $^3He/^4He$ mantle signature of the gas vents measured in the western sector of the Tiber Valley. Such a signal derives from a long-term rock–fluid interaction and limestone decarbonation favoured by high temperatures at depth. These processes lead to significantly heavier carbon isotope values than the circulation of shallower fluids, where CO_2 shows a biogenic signature mostly due to soil development and interaction. This heavy signature has been significantly overlooked in the literature, where different studies attest to this characteristic feature of the *Lapis Tiburtinus* travertine succession but never particularly focus on it.

However, despite the general signature, the analysed Sn1 and Sn2 cores record cyclical shifts, which, according to Anzalone et al.

(2017), can be correlated with global Milankovitch cycles and thus with palaeoclimate changes (Ruddiman, 2003; Shackleton et al., 2003; Ruddiman, 2006). According to Anzalone et al. (2017), a 30-m-thick travertine-core drilled in the north-western sector of the Acque Albule Basin shows a stacking pattern of the *Lapis Tiburtinus* travertine succession characterized by a hierarchy of higher to lower frequency cycles. Such a pattern is controlled and influenced by millennial-scale solar perturbations (i.e., short-term cycles) to sub-Milankovitch (i.e., medium-term cycles) and Milankovitch (i.e., long-term cycles) periodicities. Anzalone et al. (2017) suggest that the higher cycles are related to water table fluctuations associated with millennial-scale climatic changes and solar perturbation, while the lower-frequency cycles are associated with medium- and longer-term precession-driven periodicities. Moreover, according to Anzalone et al. (2017), this hypothesis is also justified by the hierarchical organization of the travertine shown in the travertine depositional units, affected only by discontinuous surfaces observable both along the quarry walls and in the analysed cores. Nevertheless, the hydrothermal origin of the travertines obviously masks the precise water temperature changes related to climatic shifts, as compared to the marine limestones usually investigated in this context. However, a potential climatic control, among the endogenic ones, on the travertine deposition has already been found by different studies and based on sedimentological organization and stable isotope values (Faccenna et al., 2008; Anzalone et al., 2017; Castorina et al., 2023). As already found by Dabkowski and Limondin-Lozouet (2022) and by Sancho et al. (2015), the calcareous tufa deposits are able to record climatic conditions, especially during the Holocene and Pleistocene. Stage MIS5 was particularly characterized by warmer and wetter conditions than today (Sancho et al., 2015). Although the examples described by previous research are not travertine deposits but calcareous tufa, the example described in the Denizli area in Turkey is representative of travertine deposits. According to Özkul et al. (2013), these deposits, coeval with the *Lapis Tiburtinus* travertine, are independent of climatic changes, and the most important controlling factor is represented by tectonic activity. As also observed by Faccenna et al. (2008), the *Lapis Tiburtinus* travertine and the Acque Albule Basin are controlled by tectonic activity. However, Mancini et al. (2021) suggested that the *Lapis Tiburtinus* travertine deposits, while influenced by tectonic activity, are also mainly influenced and controlled by climate changes. In this view, tectonic activity controls only the location of the spring at basin scale. For these reasons, the Denizli Basin and the Acque Albule Basin travertine deposits (*Lapis Tiburtinus*) are, in our opinion, comparable only in terms of depositional conditions, lithofacies, and geobody geometries.

Three main controlling factors and processes are addressed below: 1) Pleistocene glacial-interglacial cyclicity, and the MIS-5 record in particular; 2) the alternation of arid and humid phases; 3) changes in the groundwater table height and its influence on CO_2 degassing.

5.1 The MIS-5 record

In this framework, in fact, the two Sn1 and Sn2 cores record isotopic shifts that represent the precessional cyclicity identified during the warm MIS-5 (Figure 5A). The Sn1 core records two positive oxygen (5d and 5b) and two negative oxygen (5c and 5a) shifts, respectively, indicative of cool and warm sub-Milankovitch cycles between 115 and 50 Ka (Shackleton, 1969; Ruddiman, 2006). The Sn2 core, instead, records only 5c and 5a warm phases, separated by the 5b oxygen shift towards less depleted values, which identifies a colder phase (Figure 5A). Interestingly, similar shifts have been recorded and observed in two palaeo-lacustrine carbonate records of Central Italy (Fucino and Sulmona lake records) (Giaccio et al., 2015; Regattieri et al., 2015), attesting to the overall regional climatic sensitivity of the Central Apennines during the Late Pleistocene. The climatic control on these shifts is also demonstrated by the fact that they are present in both cores despite the relative distance from the springs and the different lithofacies.

5.2 Influence of arid and humid conditions

However, despite the overall precessional control from which is inferred the pace of these shifts, several superimposed controlling factors might have played a role in determining the recorded oxygen isotope signature. In fact, peak 5d in Sn1 results in a much wider peak than the second positive peak since it developed during an arid period (Figure 5A; Tzedakis et al., 2001). Arid conditions favour evaporation and also attest to low meteoric precipitation rates, which would lower the oxygen isotope ratios in carbonate precipitates. Conversely, peak 5b corresponds to the less depleted shift recorded in the Sn2 core within laminated deposits and crystalline crust lithofacies. In this case, the regional pollen records of Magri (1989) and Tzedakis et al. (2001) attest to overall humid conditions, but the facies in which the widest shift is recorded are those more controlled by evaporation and fast degassing processes.

Therefore, the oxygen isotope record of this complex travertine system proved to be better controlled by cyclic climate shifts, but numerous local factors, such as the influence of meteoric waters, stagnation, movement, and the depth of the supersaturated fluids from which travertines precipitated, acted to hamper or enhance global trends.

5.3 Influence of the groundwater table on CO_2 degassing

Carbon isotope ratios of travertines are mostly controlled by degassing and interaction with organic matter, which affects fractionation with both photosynthesis and respiration. CO_2 degassing deprives the water of light ^{12}C, leaving inorganic carbonates relatively enriched in the heavy ^{13}C isotope (Pentecost, 2005; Kele et al., 2008; Della Porta, 2015). In the analysed cores (Figure 5B), two positive carbon isotope shifts can be identified. The first, in Sn1, is recorded within non-laminated deposits during the cool and arid 5d phase, as attested by the pollen record of the Castiglione Crater site, located 10 km from the Acque Albule Basin (Tzedakis et al., 2001). In this case, this positive carbon isotope signature is likely mostly controlled by the arid climate phase which determined the lowering of the groundwater table and the enhancement of light CO_2 degassing. Conversely, the
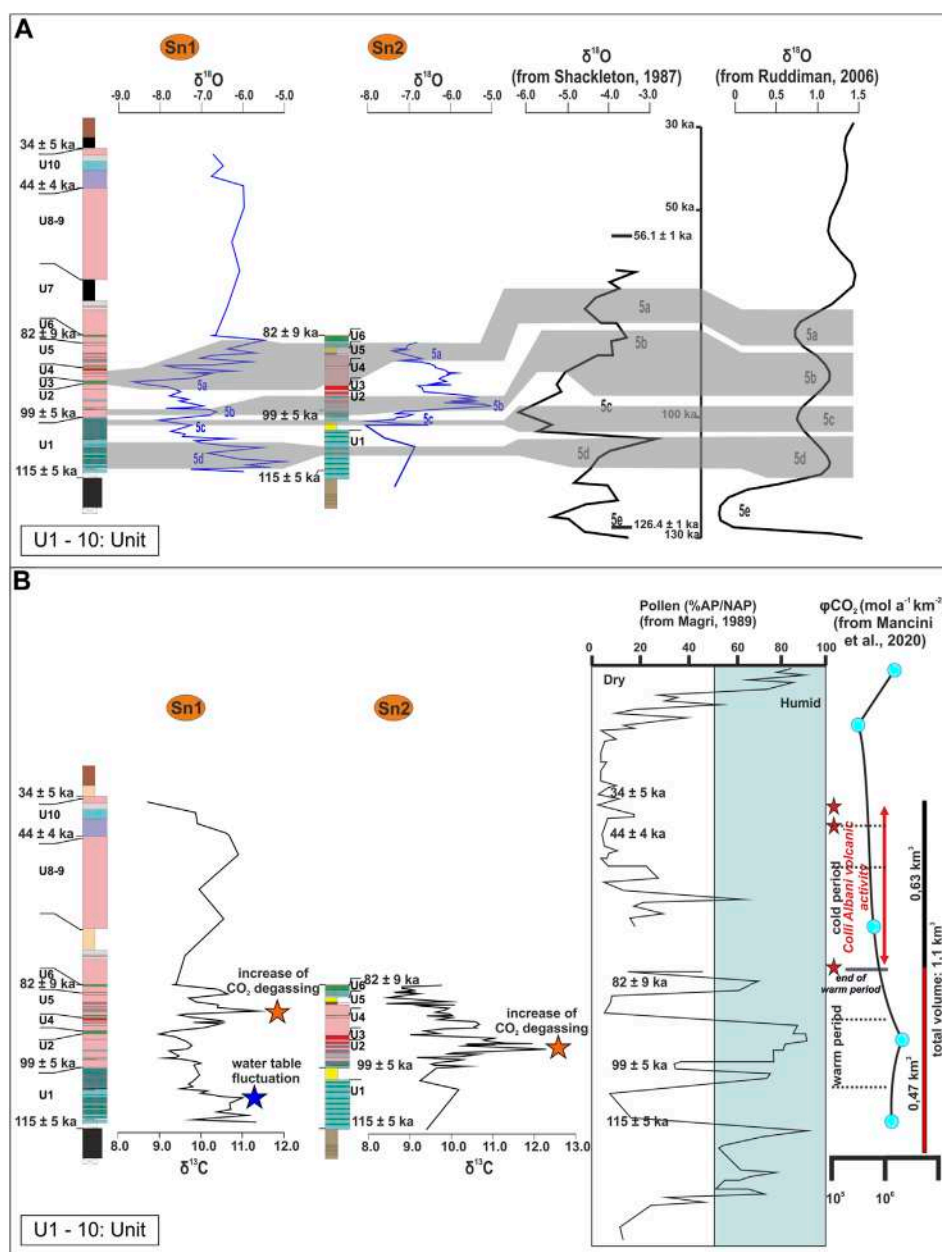
FIGURE 5
(A) Oxygen isotope ratios of the Sn1 and Sn2 cores correlated with climate curves reconstructed by Shackleton (1987) and Ruddiman (2006). The oxygen isotope curve of Sn2 shows less depleted (5d and 5b) and more depleted (5c and 5a) shifts related to cool and warm sub-Milankovitch cycles of 115−50 Ka. The Sn1 oxygen isotope curves reconstructed instead show only 5c and 5a warm phases, separated by the 5b oxygen less depleted shift and related to a cold phase. **(B)** Carbon isotope curves of Sn1 and Sn2 correlated with pollen stratigraphy of the Castiglione Crater (Magri, 1989; Tzedakis et al., 2001) and CO$_2$ fluxes calculated for the depositional units of the *Lapis Tiburtinus* travertine succession. Carbon isotope variations are interpreted to relate to water table fluctuations and increased CO$_2$ degassing associated with the Colli Albani volcanic complex activity.

second positive carbon isotope shift, recorded within laminated deposits of the Sn2 core, occurred during the 5b cool phase; unlike the 5d, this attests to increased humid conditions in Central Italy (Tzedakis et al., 2001). However, it recorded a moment of increased CO$_2$ degassing in the *Lapis Tiburtinus* travertine systems (Mancini et al., 2020). The *Lapis Tiburtinus* travertine deposition commenced after the beginning of the warm period (isotopic stage 5) from 115 ka, and its end coincided with the cold and dry

period related to isotopic stage 2 about 30 ka (Faccenna et al., 2008). Mantle degassing phenomena, a variation of CO$_2$ fluxes associated with the *Lapis Tiburtinus* travertine deposition, occurred in the last 115 ka and can be associated with the Colli Albani volcanic complex, as already indicated by Mancini et al. (2020). In fact, the variation in travertine deposition could be influenced by climatic changes, thus affecting changes in deposition rates due to varied CaCO$_3$ solubility in the amount of water available in the aquifer
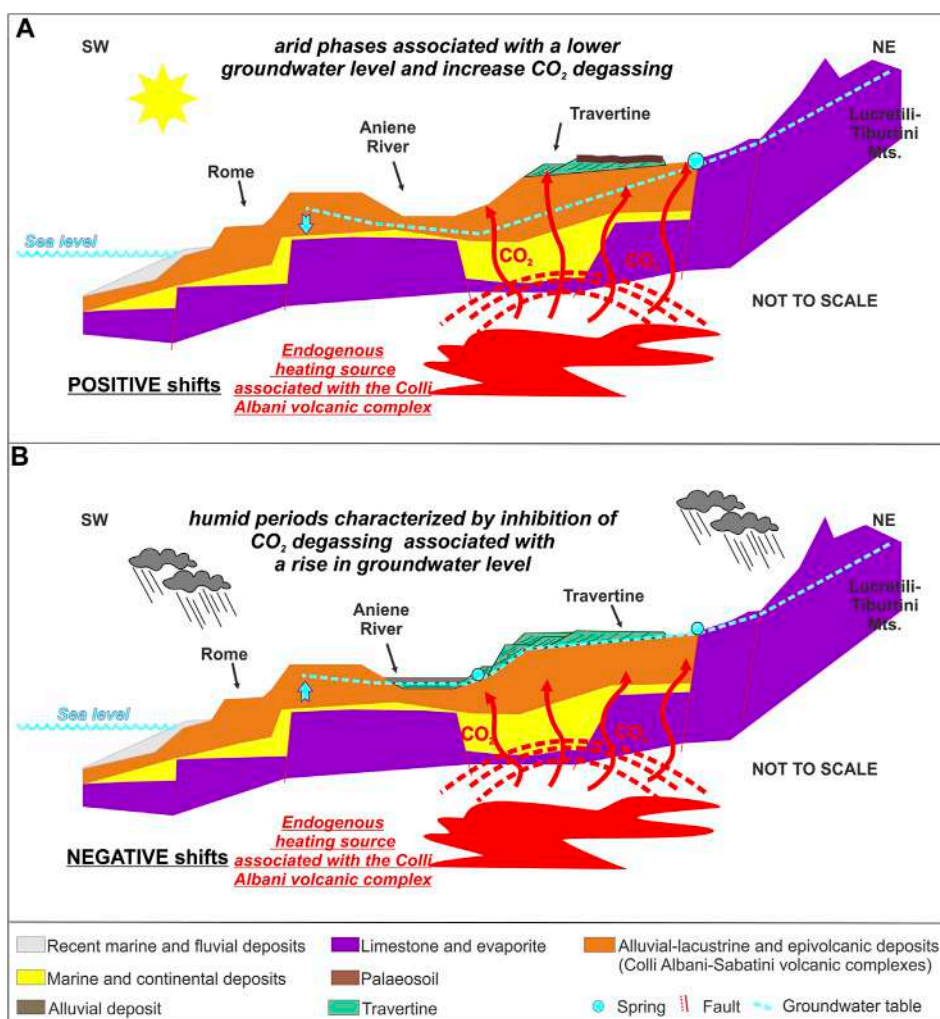
FIGURE 6
Schematic model showing the possible cause of the carbon isotope shifts measured for the *Lapis Tiburtinus* travertine succession. The positive shifts are associated with arid phases, with a low groundwater level leading to an increase in CO_2 degassing phenomena **(A)**, while the humid periods are characterized by inhibited CO_2 degassing associated with a groundwater level rise **(B)** (modified from Mancini et al., 2021).

(Figure 6) and by changes in the deep flux of CO_2. Travertine volume variations and the related calculated CO_2 fluxes reveal that, within a warm period, some larger depositional hiatus followed by a continuous travertine deposition and CO_2-associated flux occurred (82–44 ka). Instead, at the end of a cold period, travertine deposition and associated CO_2 fluxes increase. Such an increase, occurring between 44 and 30 ka, cannot be justified by significant climatic variation, as also demonstrated by the pollen content measured in the Castiglione Crater which is similar to previous periods (Magri, 1989). The calculated volume and associated CO_2 flux more than doubled compared to the previous period, which is likely related to variations in the water table and a changed degassing rate related to the Colli Albani volcanic activity. Moreover, the maximum CO_2 degassing activity (2.70×10^6 mol a^{-1} km^{-2}) associated with travertine deposition occurred 44 to 30 ka, which also corresponds with the last phase of volcanic activity in the Colli Albani volcanic complex (56.5 ka–30 ka) (De Rita et al., 1995, De Rita et al., 2002; Gaeta et al., 2000; Karner et al., 2001; Giordano et al., 2010).

Increased degassing controlled an increased fractionation effect of the carbon isotopes and relative enrichment of the heavier isotope in the supersaturated fluids. Furthermore, humid conditions might have controlled organic matter blooms and soil developments, which could also have led to enhanced carbon isotope fractionation. In this framework, laminated deposits, strongly influenced by evaporation, are less prone to organic matter blooms than other facies, such as non-laminated deposits characterised by higher water depth and stagnation, or soils. Obviously, the extreme latter variation of travertine facies in a relatively small space hampers the possibility of correlating all the isotopic shifts at a basin-scale level, but it does provide useful insights into the overall carbon cycle dynamics in such a complex environment (Figure 6). Moreover, Brasier et al. (2011) suggested that the primary $\delta^{18}O$ values can be altered due to dissolution and reprecipitation phenomena, especially if these processes occurred in fluids with different temperatures and/or compositions, leading finally to an isotopic homogenization of the bulk stable isotopes and removal of
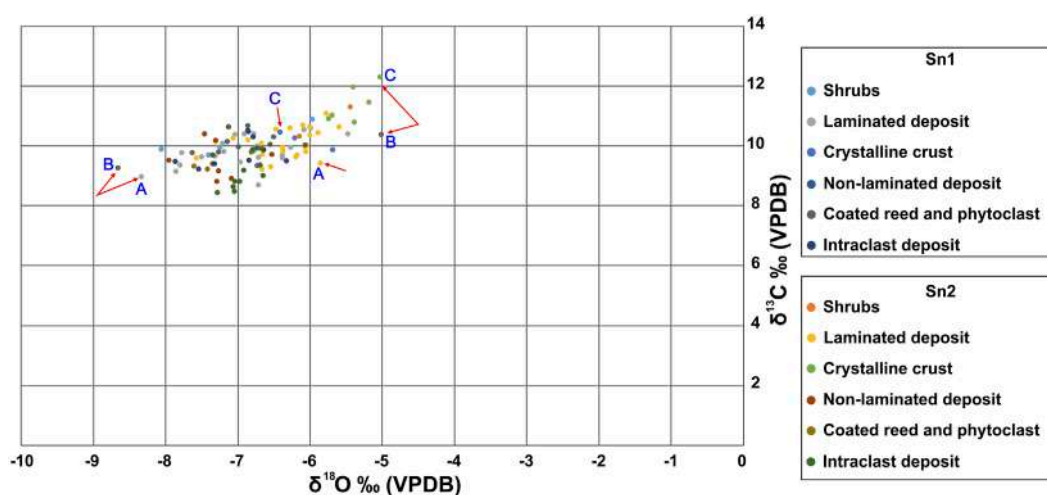
FIGURE 7
Boxplot showing the relationship between carbon and oxygen stable isotopes measured in the Sn1 and Sn2 cores, displaying some correlation. However, some value shifts are observable (see values indicated by A, B, and C). "A" values are representative of "laminated deposit lithofacies," developed in a low-energy setting affected by evaporation. The "B" value relates to "coated reed and phytoclast lithofacies," attesting to some stagnant environmental conditions affected by freshwater input. Such a shift could be indicative of a biotic effect. The "C" value is instead indicative of "crystalline crust lithofacies," attesting to a high-energy setting characterized by rapid degassing phenomena. In this view, as also reported in Brasier et al. (2011), a limited diagenetic effect could have influenced the travertine deposits of the *Lapis Tiburtinus*.

differences between micrite and sparite stable isotopes (Allan and Matthews, 1982; Beck et al., 2005; Watkins et al., 2014). However, the differences between oxygen-stable isotopic values of the cement and micrite of most samples, tested before sample preparation and analysis, are significantly large, implying at least partial preservation of the isotopic signatures. Carbon isotopic signature instead possesses a better preservation potential due to carbon buffering (Brasier et al., 2011). In this view, the $\delta^{13}C$ signatures are the result of continuous re-equilibration with new fluids, starting from syn-depositional conditions (Erthal et al., 2017; Daëron et al., 2019). Consequently, due to the limited time available for the Late Pleistocene–Holocene (Faccenna et al., 2008) cementation of this deposit, the diagenetic resetting is considered relatively minor (Figure 7).

In summary, this record shows that the fractionation of carbon isotopes in travertine systems is far more complex than in other carbonate systems and is related to multiple factors which are not always easily detectable. However, this record shows that positive carbon isotope shifts occur preferentially during relatively cold phases and high CO_2 degassing.

6 Conclusion

This study demonstrates that travertine precipitation is controlled by a complex set of physical, chemical, and biological processes and is marked by the overall heterogeneity of facies even over small distances. However, the detailed analysis of stable C- and O-isotope records from travertine deposits can still provide insights into the sensitivity of travertine systems to climate changes and into the relationship between the global, regional, and local controlling factors of their deposition. The

stable isotope record of the analysed cores testifies to a travertine system sensitive to global climate changes, the signature of which was only partially hampered by local factors. The oxygen isotope record, on the one hand, can be correlated with precessional cycles within the warm MIS5 stage even if evaporation processes significantly amplify the wideness of the shifts. On the other hand, the carbon isotope ratios are mostly controlled by CO_2 degassing. When the latter increases, either due to endogenic factors or reduced pressure in the aquifer during arid phases, the fractionation effect among carbon isotopes increases, leading to a major degassing of light carbon in the atmosphere and relative enrichment in heavy ^{13}C in the inorganic carbonate. In this view, travertine deposits, largely used to constrain and reconstruct the tectonic activity of the area where they develop, could also be used as a proxy to investigate climatic changes and groundwater table variations based on variations in oxygen and carbon stable isotopes.

Data availability statement

The raw data supporting the conclusion of this article will be made available by the authors, without undue reservation.

Author contributions

AM: conceptualization, investigation, supervision, and writing–original draft. IC: conceptualization, methodology, validation, and writing–original draft. JL: data curation, investigation, and writing–original draft. EC: supervision,

validation, and writing–review and editing. RS: project administration, resources, supervision, validation, and writing–review and editing. MB: conceptualization, visualization, and writing–review and editing.

Funding

The authors declare that financial support was received for the research, authorship, and/or publication of this article. Financial support was received for the research activity from Shell, Total, and Petrobras in the frame of the TraRAS project. The funders were not involved in the study design, collection, analysis, interpretation of data, the writing of this article, or the decision to submit it for publication.

Conflict of interest

The authors declare that the research was conducted in the absence of any commercial or financial relationships that could be construed as a potential conflict of interest.

Publisher's note

All claims expressed in this article are solely those of the authors and do not necessarily represent those of their affiliated organizations or those of the publisher, the editors, and the reviewers. Any product that may be evaluated in this article, or claim that may be made by its manufacturer, is not guaranteed or endorsed by the publisher.

References

Acocella, V., and Funiciello, R. (2006). Transverse systems along the extensional tyrrhenian margin of Central Italy and their influence on volcanism. *Tectonics* 25, TC2003. doi:10.1029/2005tc001845

Allan, J. R., and Matthews, R. K. (1982). Isotope signatures associated with early meteoric diagenesis. *Sedimentology* 29, 797–817. doi:10.1111/j.1365-3091.1982.tb00085.x

Anzalone, E., and D'ArgenioFerreri, B. V. (2017). Depositional trends of travertines in the type area of Tivoli (Italy). *Rend. Fis. Acc. Lincei* 28, 341–361. doi:10.1007/s12210-017-0595-1

Beck, W. C., Grossmann, E. L., and Morse, J. W. (2005). Experimental studies of oxygen isotope fractionation in the carbonic acid system at 15°, 25°, and 40°C. *Geochimica Cosmochimica Acta* 69 (14), 3493–3503. doi:10.1016/j.gca.2005.02.003

Billi, A., Tiberti, M. M., Cavinato, G. P., Cosentino, D., Di Luzio, E., Keller, J. V. A., et al. (2006). First results from the CROP-11 deep seismic profile, central Apennines, Italy: evidence of mid-crustal folding. *J. Geol. Soc.* 163, 583–586. doi:10.1144/0016-764920-002

Brasier, A. T., Andrews, J. E., and Ckendall, A. C. (2011). Diagenesis or dire genesis? The origin of columnar spar in tufa stromatolites of central Greece and the role of chironomid larvae. *Sedimentology* 58, 1283–1302. doi:10.1111/j.1365-3091.2010.01208.x

Brogi, A., Alçiçek, M. C., Liotta, D., Capezzuoli, E., Zucchi, M., and Matera, P. F. (2021a). Step-over fault zones controlling geothermal fluid-flow and travertine formation (Denizli Basin, Turkey). *Geothermics* 89, 101941. doi:10.1016/j.geothermics.2020.101941

Brogi, A., Capezzuoli, E., Aqué, R., Branca, M., and Voltaggio, M. (2010). Studying travertines for neotectonics investigations: middle-late Pleistocene syntectonic travertine deposition at serre di Rapolano (northern Apennines, Italy). *Int. J. Earth Sci.* 99, 1383–1398. doi:10.1007/s00531-009-0456-y

Brogi, A., Capezzuoli, E., Karabacak, V., Alçiçek, M. C., and Luo, L. (2021b). Fissure ridges: a reappraisal of faulting and travertine deposition (travitonics). *Geosciences* 11, 278. doi:10.3390/geosciences11070278

Brogi, A., Capezzuoli, E., Moretti, M., Olvera-Garcia, E., Matera, P. F., Garduno-Monroy, V. H., et al. (2018). Earthquake-triggered soft-sediment deformation structures (seismites) in travertine deposits. *Tectonophysics* 745, 349–365. doi:10.1016/j.tecto.2018.08.021

Capezzuoli, E., Gandin, A., and Pedley, M. (2014). Decoding tufa and travertine (fresh water carbonates) in the sedimentary record: the state of the art. *Sedimentology* 61, 1–21. doi:10.1111/sed.12075

Cardello, G. L., Tomassetti, L., Cornacchia, I., Mancini, A., Mancini, M., Mazzini, I., et al. (2022). The Tethyan and Tyrrhenian margin record of the Central Apennines: a guide with insights from stratigraphy, tectonics, and hydrogeology. *Geol. F. Trips Maps* 14 (2), 1–113. doi:10.3301/GFT.2022.05

Carucci, V., Petitta, M., and Aravena, R. (2012). Interaction between shallow and deep aquifers in the Tivoli Plain (Central Italy) enhanced by groundwater extraction: a multi isotope approach and geochemical modelling. *Appl. Geochem.* 27, 266–280. doi:10.1016/j.apgeochem.2011.11.007

Castorina, F., Masi, U., Billi, A., De Filippis, L., and Nisi, S. (2023). Elemental and Sr–Nd isotopic evidence for unravelling the origin of the low-temperature geothermal fluids of Tivoli Terme (Latium, central Italy) between erosional S4 and S3 phases (upper Pleistocene) and neotectonics implications. *Appl. Geochem.* 158, 105794. doi:10.1016/j.apgeochem.2023.105794

Chafetz, H. S., and Folk, R. L. (1984). Travertines: depositional morphology and the bacterially constructed constituents. *J. Sediment. Res.* 54, 289–316. doi:10.1306/212f8404-2b24-11d7-8648000102c1865d

Chiodini, G., Cardellini, C., Amato, A., Boschi, E., Caliro, S., Frondini, F., et al. (2004). Carbon dioxide Earth degassing and seismogenesis in central and southern Italy. *Geophys. Res. Lett.* 31, 1–4. doi:10.1029/2004G.L019480

Claes, H., Degros, M., Soete, J., Claes, S., Kele, S., Mindszenty, A., et al. (2016). Geobody architecture, genesis and petrophysical characteristics of the Budakalász travertines, Buda Hills (Hungary). *Quat. Int.* 437, 107–128. doi:10.1016/j.quaint.2016.09.007

Claes, H., Soete, J., Van Noten, K., El Desouky, H., Erthal, M. M., Vanhaecke, F., et al. (2015). Sedimentology, three-dimensional geobody reconstruction and carbon dioxide origin of Pleistocene travertine deposits in the Ballık area (south-west Turkey). *Sedimentology* 62, 1408–1445. doi:10.1111/sed.12188

Conato, V., Esu, D., Malatesta, A., and Zarlenga, F. (1980). New data on the Pleistocene of Rome. *Quaternaria* 22, 131–176.

Corrado, S., Cosentino, D., Crescenzi, B., and Parotto, M. (1992). Geometrie delle deformazioni della Sabina meridionale attraverso la ricostruzione di superfici strutturali (Lazio, Appennino Centrale). *Studi Geol. Camerti* 1991, 47–53. doi:10.15165/studgeocam-1405

Cosentino, D., and Parotto, M. (1986). Assetto strutturale dei Monti Lucretili settentrionali (Sabina): nuovi dati e schema tettonico preliminare. *Geol. Romana* 25, 73–90.

Crossey, L. J., Fischer, T. P., Patchett, P. J., Karlstrom, K. E., Hilton, D. R., Newell, D. L., et al. (2006). Dissected hydrologic system at the Grand Canyon: interaction between deeply derived fluids and plateau aquifer waters in modern springs and travertine. *Geology* 34, 25–28. doi:10.1130/G22057.1

Dabkowski, J., and Limondin-Lozouet, N. (2022). Comparison of temperature and humidity during MIS 11 and MIS 5e interglacials with the Holocene using stable isotopes in tufa deposits from northern France. *Quat. Res.* 107, 147–158. doi:10.1017/qua.2021.66

Daëron, M., Drysdale, R. N., Peral, M., Huyghe, D., Blamart, D., Coplen, T. B., et al. (2019). Most Earth-surface calcites precipitate out of isotopic equilibrium. *Nat. Commun.* 10, 429. doi:10.1038/s41467-019-08336-5

De Filippis, L., Anzalone, E., Billi, A., Faccenna, C., Poncia, P. P., and Sella, P. (2013). The origin and growth of a recently active fissure ridge travertine over a seismic fault, Tivoli, Italy. *Geomorphology* 195, 13–26. doi:10.1016/j.geomorph.2013.04.019

Della Porta, G. (2015). "Carbonate build-ups in lacustrine, hydrothermal and fluvial settings: comparing depositional geometry, fabric types and geochemical signature," in *Microbial carbonates in space and time: implications for global exploration and production* (London: Geological Society). Special Publications 418. doi:10.1144/SP418.4

Della Porta, G., Capezzuoli, E., and De Bernardo, A. (2017a). Facies character and depositional architecture of hydrothermal travertine slope aprons (Pleistocene, Acquasanta Terme, Central Italy). *Mar. Petroleum Geol.* 87, 171–187. doi:10.1016/j.marpetgeo.2017.03.014

Della Porta, G., Croci, A., Marini, M., and Kele, S. (2017b). Depositional architecture, facies character and geochemical signature of the Tivoli travertines (Pleistocene, Acque Albule Basin, Central Italy). *Riv. Ital. Paleontol. Stratigr.* 123, 487–540. doi:10.13130/2039-4942/9148

De Rita, D., Faccenna, C., Funiciello, R., and Rosa, C. (1995). "Structural and geological evolution of the Colli Albani volcanic district," in *The volcano of the albani hills*. Editor R. Trigila (Roma: Tipografia SGS), 267–283.

De Rita, D., Giordano, G., Esposito, A., Fabbri, M., and Rodani, S. (2002). Large volume phreatomagmatic ignimbrites from the Colli Albani volcano (Middle Pleistocene, Italy). *J. Volcanol. Geotherm. Res.* 118, 77–98. doi:10.1016/S0377-0273(02)00251-2

Di Nezza, M., Cecchini, F., Margottini, S., and Di Filippo, M. (2015). *Assetto geologico strutturale profondo del Bacino delle Acque Albule (Roma, Lazio)*. Italy: Memorie Descrittive della Carta Geologica d'Italia, 267–272.

Di Salvo, C., Mazza, R., and Capelli, G. (2013). Gli acquiferi in travertino del Lazio: schemi idrogeologici e caratteristiche chimico-fisiche. *Rendiconti Online della Soc. Geol. Ital.* 27, 54–76. doi:10.3301/ROL.2013.20

Erthal, M. M., Capezzuoli, E., Mancini, A., Claes, H., Soete, J., and Swennen, R. (2017). Shrub morpho-types as indicator for the water flow energy –Tivoli travertine case (Central Italy). *Sediment. Geol.* 347, 79–99. doi:10.1016/j.sedgeo.2016.11.008

Faccenna, C., Funiciello, R., Montone, P., Parotto, M., and Voltaggio, M. (1994). Late Pleistocene strike-slip tectonics in the Acque Albule Basin (Tivoli, latium). *Mem. Descr. della Carta Geol. d'Italia* 49, 37–50.

Faccenna, C., Soligo, M., Billi, A., De Filippis, L., Funiciello, R., Rossetti, C., et al. (2008). Late Pleistocene depositional cycles of the Lapis Tiburtinus travertine (Tivoli, Central Italy): possible influence of climate and fault activity. *Glob. Planet. Change* 63, 299–308. doi:10.1016/j.gloplacha.2008.06.006

Frank, N., Braum, M., Hambach, U., Mangini, A., and Wagner, G. (2000). Warm period growth of travertine during the last interglaciation in Southern Germany. *Quat. Res.* 54, 38–48. doi:10.1006/qres.2000.2135

Funiciello, R., Locardi, E., and Parotto, M. (1976). Lineamenti geologici dell'area sabatina orientale. *Boll. della Soc. Geol. Ital.* 95, 831–849.

Gaeta, M., Fabrizio, G., and Cavarretta, G. (2000). F-phlogopites in the Alban Hills Volcanic District (Central Italy): indications regarding the role of volatiles in magmatic crystallisation. *J. Volcanol. Geotherm. Res.* 99, 179–193. doi:10.1016/S0377-0273(00)00172-4

Gasparini, C., Di Maro, R., Pagliuca, N., Pirro, M., and Marchetti, A. (2002). Recent seismicity of the "Acque Albule" travertine basin. *Ann. Geophys.* 45, 537–550. doi:10.4401/ag-3521

Giaccio, B., Regattieri, E., Zanchetta, G., Nomade, S., Renne, P. R., Sprain, C. J., et al. (2015). Duration and dynamics of the best orbital analogue to the present interglacial. *Geology* 43 (7), 603–606. doi:10.1130/g36677.1

Giordano, G., De Benedetti, A., Diana, A., Diano, A., Esposito, A., Fabbri, M., et al. (2010). *Stratigraphy, volcano tectonics and evolution of the Colli Albani volcanic field. Volume 3: the Colli Albani volcano*. London: Iavcei, 276.

Giustini, F., Brilli, M., Di Salvo, C., Mancini, M., and Voltaggio, M. (2020). Multidisciplinary characterization of the buried travertine body of Prima Porta (Central Italy). *Quat. Int.* 568, 65–78. doi:10.1016/j.quaint.2020.10.062

Hancock, P. L., Chalmers, R. M. L., Altunel, E., and Çakır, Z. (1999). Travitonics: using travertines in active fault studies. *J. Struct. Geol.* 21, 903–916. doi:10.1016/S0191-8141(99)00061-9

Jones, B., and Renaut, R. W. (2010). "Calcareous spring deposits in continental setting," in *Carbonates in continental settings – facies, Environments and processes*. Editors A. M. Alonso-Zarza, and L. H. Tanner (Elsevier: Developments in sedimentology) 61, 177–224. doi:10.1016/S0070-4571(09)06104-4

Karner, D. B., Marra, F., and Renne, P. R. (2001). The history of the monti sabatini and alban hills volcanoes: groundwork for assessing volcanic-tectonic hazards for Rome. *J. Volcanol. Geotherm. Res.* 107, 185–219. doi:10.1016/S0377-0273(00)00258-4

Kele, S., Demény, A., Siklósy, Z., Németh, T., Tóth, M., and Kovács, M. B. (2008). Chemical and stable isotope composition of recent hot-water travertines and associated thermal waters, from Egerszalók, Hungary: depositional facies and non-equilibrium fractionation. *Sediment. Geol.* 211, 53–72. doi:10.1016/j.sedgeo.2008.08.004

La Vigna, F., Mazza, R., and Capelli, G. (2013a). Le risorse idriche nei travertini della piana di Tivoli-Guidonia. La modellazione numerica come strumento di gestione degli acquiferi. *Rendiconti Online della Soc. Geol. Ital.* 27, 77–85. doi:10.3301/ROL.2013.21

La Vigna, F., Mazza, R., and Capelli, G. (2013b). Detecting the flow relationships between deep and shallow aquifers in an exploited groundwater system, using long-term monitoring data and quantitative hydrogeology: the Acque Albule basin case (Rome, Italy). *Hydrol. Processes* 27, 3159–3173. doi:10.1002/hyp.9494

Magri, D. (1989). Interpreting long-term exponential growth of plant populations in a 250000-year pollen record from Valle di Castiglione (Roma). *New Phytol.* 112, 123–128. doi:10.1111/j.1469-8137.1989.tb00317.x

Mancini, A., and Capezzuoli, E. (2024). Travertine depositional systems of Central Italy: rapolano Terme and the Acque Albule Basin. An overview of geometries and lithofacies associations of the depositional setting. *Geol. F. Trips Maps* 16 (1), 1–35. doi:10.3301/GFT.2024.03

Mancini, A., Capezzuoli, E., Brogi, A., Swennen, R., Ricci, L., and Frondini, F. (2020). Geogenic CO_2 flux calculations from the late Pleistocene Tivoli travertines (Acque Albule Basin, Tivoli, Central Italy). *Ital. J. Geosci.* 139 (3), 374–382. doi:10.3301/ijg.2020.10

Mancini, A., Capezzuoli, E., Erthal, M., and Swennen, R. (2019a). Hierarchical approach to define travertine depositional systems: 3D conceptual morphological model and possible applications. *Mar. Petroleum Geol.* 103, 549–563. doi:10.1016/j.marpetgeo.2019.02.021

Mancini, A., Della Porta, G., Swennen, R., and Capezzuoli, E. (2021). 3D reconstruction of the *Lapis Tiburtinus* (Tivoli, Central Italy): the control of climatic and sea-level changes on travertine deposition. *Basin Res.* 33 (5), 2605–2635. doi:10.1111/bre.12576

Mancini, A., Frondini, F., Capezzuoli, E., Galvez Mejia, E., Lezzi, G., Matarazzi, D., et al. (2019b). Evaluating the geogenic CO_2 flux from geothermal areas by analysing quaternary travertine masses. New data from western central Italy and review of previous CO_2 flux data. *Quat. Sci. Rev.* 215, 132–143. doi:10.1016/j.quascirev.2019.04.030

Mancini, A., Frondini, F., Capezzuoli, E., Galvez Mejia, E., Lezzi, G., Matarazzi, D., et al. (2019c). Porosity, bulk density and CaCO3 content of travertines. A new dataset from Rapolano, Canino and Tivoli travertines (Italy). *Data brief* 25, 104158–158. doi:10.1016/j.dib.2019.104158

Mancini, M., Marini, M., Moscatelli, M., Pagliaroli, A., Stigliano, F., Di Salvo, C., et al. (2014). A physical stratigraphy model for seismic microzonation of the Central Archaeological Area of Rome (Italy). *Bull. Earthq. Eng.* 12, 1339–1363. doi:10.1007/s1051.8-014-9584-2

Minissale, A. (2004). Origin, transport and discharge of CO_2 in Central Italy. *Earth Sci. Rev.* 66, 89–141. doi:10.1016/j.earscirev.2003.09.001

Minissale, A., Kerrick, D. M., Magro, G., Murrell, M. T., Paladini, M., Rihs, S., et al. (2002). Geochemistry of Quaternary travertines in the region north of Rome (Italy): structural, hydrologic, and paleoclimatic implications. *Earth Planet. Sci. Lett.* 203, 709–728. doi:10.1016/S0012-821X(02)00875-0

Özkul, M., Kele, S., Gökgöz, A., Shen, C. C., Jones, B., Baykara, M. O., et al. (2013). Comparison of the Quaternary travertine sites in the Denizli extensional basin based on their depositional and geochemical data. *Sediment. Geol.* 294, 179–204. doi:10.1016/j.sedgeo.2013.05.018

Pedley, H. M. (2009). Tufas and travertines of the Mediterranean region: a testing ground for freshwater carbonate concepts and developments. *Sedimentology* 56, 221–246. doi:10.1111/j.1365-3091.2008.01012.x

Pentecost, A. (2005). *Travertine*. Heidelberg: Springer. ISBN: 1 40203523 3.

Pentecost, A., and Tortora, C. (1989). Bagni di Tivoli, Lazio: a modern travertine depositing site and its associated microorganisms. *Boll. della Soc. Geol. Ital.* 108, 315–324.

Regattieri, E., Giaccio, B., Zanchetta, G., Drysdale, R. N., Galli, P., Nomade, S., et al. (2015). Hydrological variability over the Apennines during the Early Last Glacial precession minimum, as revealed by a stable isotope record from Sulmona Basin, Central Italy. *J. Quat. Sci.* 30, 19–31. doi:10.1002/jqs.2755

Ricketts, J. W., Ma, L., Wagler, A. E., and Garcia, V. H. (2019). Global travertine deposition modulated by oscillations in climate. *J. Quat. Sci.* 34 (7), 558–568. doi:10.1002/jqs.3144

Ronchi, P., and Cruciani, F. (2015). Continental carbonates as a hydrocarbon reservoir, an analog case study from the travertine of Saturnia, Italy. *AAPG Bull.* 99, 711–734. doi:10.1306/10021414026

Rossetti, F., Tecce, F., Billi, A., and Brilli, M. (2007). Patterns of fluid flow in the contact aureole of the late Miocene Monte Capanne pluton (Elba Island, Italy): the role of structures and rheology. *Contributions Mineralogy Petrology* 153, 743–760. doi:10.1007/s00410-006-0175-3

Ruddiman, W. F. (2003). Orbital insolation, ice volume, and greenhouse gases. *Quat. Sci. Rev.* 22, 1597–1629. doi:10.1016/S0277-3791(03)00087-8

Ruddiman, W. F. (2006). Orbital changes and climate. *Quat. Sci. Rev.* 25, 3092–3112. doi:10.1016/j.quascirev.2006.09.001

Sancho, C., Arenas, C., Vázquez-Urbez, M., Pardo, G., Lozano, M. V., Peña-Monné, J. L., et al. (2015). Climatic implications of the Quaternary fluvial tufa record in the NE Iberian Peninsula over the last 500 ka. *Quat. Res.* 84, 398–414. doi:10.1016/j.yqres.2015.08.003

Scalera, F., Mancini, A., Capezzuoli, E., Claes, H., and Swennen, R. (2021). The Testina travertine (Acque Albule Basin, Tivoli, Central Italy): a paleoenvironmental reconstruction of a shallow hydrothermal lake depositional system. The importance of climatic variations over the Late Pleistocene. *depositional Rec.* 8 (1), 266–291. doi:10.1002/dep2.155

Schröder, S., Ibekwe, A., Saunderes, M., Dixon, R., and Fisher, A. (2016). Algal-microbial carbonates of the Namibe Basin (Albian, Angola): implications for microbial carbonate mound development in the South Atlantic. *Pet. Geosci.* 22, 71–90. doi:10.1144/petgeo2014-083

Shackleton, N. J. (1969). The last interglacial in the marine and terrestrial record. *Proc. R. Soc. Lond. B* 174, 135–154.

Shackleton, N. J. (1987). Oxygen isotopes, ice volume and sea level. *Quat. Sci. Rev.* 6 (3–4), 183–190. ISSN 0277-3791. doi:10.1016/0277-3791(87)90003-5

Shackleton, N. J., Sánchez-Goñi, M. F., Pailler, D., and Lancelot, Y. (2003). Marine Isotope Substage 5e and the Eemian Interglacial. *Glob. Planet. Change* 36 (3), 151–155. ISSN 0921-8181. doi:10.1016/S0921-8181(02)00181-9

Tarquini, S., Isola, I., Favalli, M., Battistini, A., and Dotta, G. (2023). *TINITALY, a digital elevation model of Italy with a 10 meters cell size (Version 1.1)*. Istituto Nazionale di Geofisica e Vulcanologia. doi:10.13127/tinitaly/1.1

Tzedakis, P. C., Andrieu, V., de Beaulieu, J. L., Birks, H. J. B., Crowhurst, S., Follieri, M., et al. (2001). Establishing a terrestrial chronological framework as a basis for biostratigraphical comparisons. *Quat. Sci. Rev.* 20, 1583–1592. doi:10.1016/S0277-3791(01)00025-7

Uysal, I. T., Feng, Y., Zhao, J., Altunel, E., Weatherley, D., Karabacak, V., et al. (2007). U-series dating and geochemical tracing of late Quaternary travertine in co-seismic fissures. *Earth Planet. Sci. Lett.* 257, 450–462. doi:10.1016/j.epsl.2007.03.004

Uysal, I. T., Feng, Y., Zhao, J., Isik, V., Nuriel, P., and Golding, S. D. (2009). Hydrothermal CO_2 degassing in seismically active zones during the late Quaternary. *Chem. Geol.* 265, 442–454. doi:10.1016/j.chemgeo.2009.05.011

Watkins, J. M., Hunt, J. D., Ryerson, F. J., and DePaolo, D. J. (2014). The influence of temperature, pH, and growth rate on the $\delta^{18}O$ composition of inorganically precipitated calcite. *Earth Planet. Sci. Lett.* 404, 332–343. doi:10.1016/j.epsl.2014.07.036